Three-point bending tests of notched beams: a suitable test to investigate size effect of plain concrete

Christian Carloni and Mohammod Minhajur Rahman

Case Western Reserve University, Cleveland, OH, USA

American Concrete Institute
Always advancing

ACI 380 Session:
Applications of Structural Plain Concrete

Outline

- Introduction on LEFM
- Concrete
- Size Effect
- Tests on Notched Beams
- How to model?
- Conclusions

Christian Carloni
cxc966@case.edu

Linear Elastic Fracture Mechanics

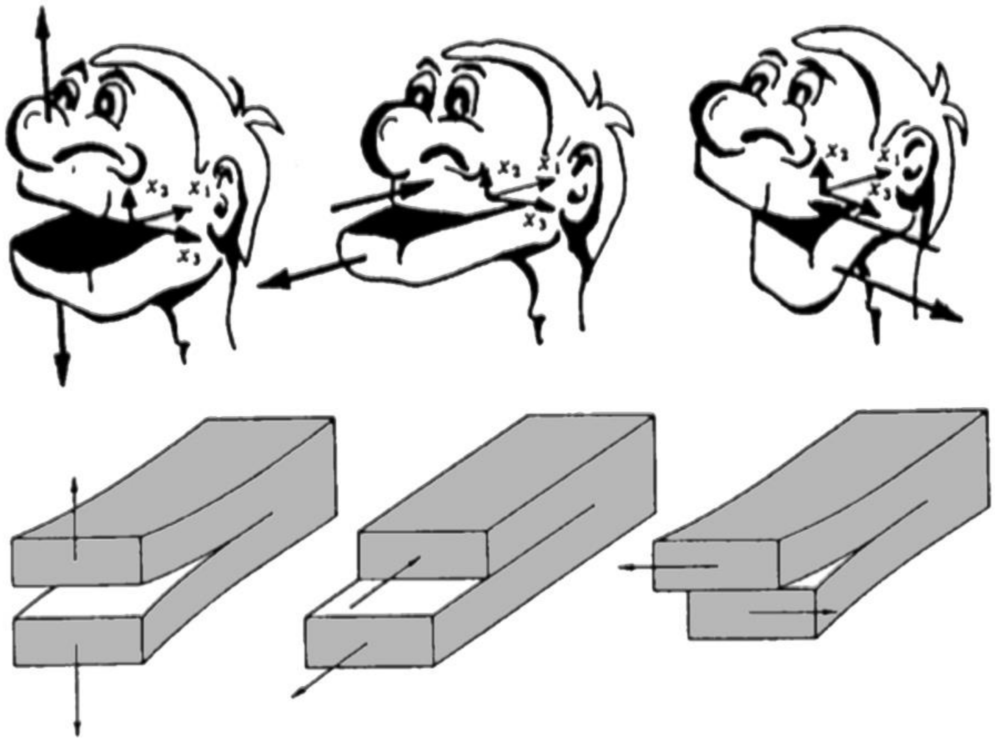

There are three types of loading that a crack can experience.

- Mode I loading tends to open the crack.
- Mode II loading tends to slide one crack face with respect to the other.
- Mode III refers to out-of-plane shear.

Christian Carloni
cxc966@case.edu

Linear Elastic Fracture Mechanics

British aeronautical engineer A. A. Griffith noticed that in presence of a crack the stress value cannot be used as a criterion of failure!

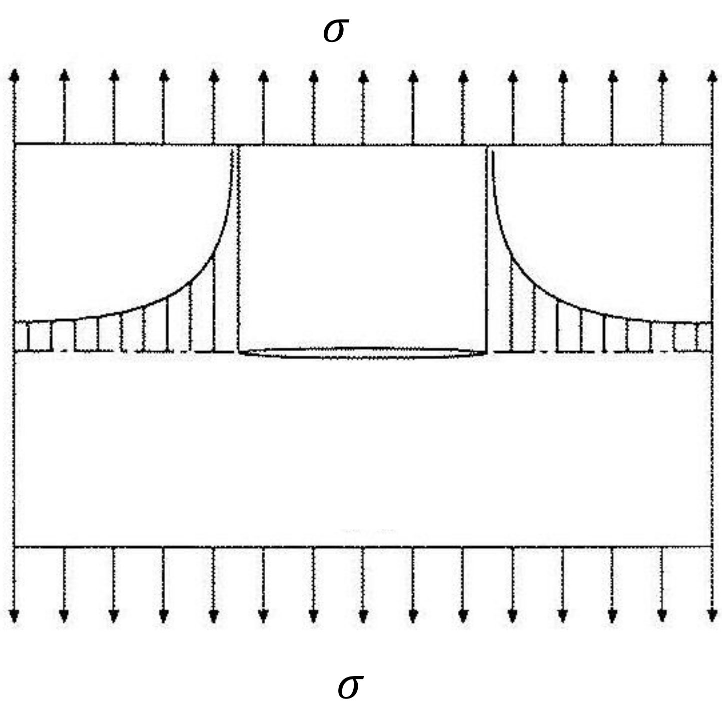

Stress perpendicular to the crack line

Stress intensity factor

$$\boxed{\sigma_{22} = \frac{K_I}{\sqrt{2\pi r}}}$$

$$\boxed{K_I = \sigma\sqrt{D}k(\alpha)}$$

When the crack propagates:

$$\boxed{K_I = K_{Ic}}$$

$$\boxed{\sigma = \sigma_N}$$

Cohesive Crack Model

In its simplest form the cohesive crack model was introduced by Barenblatt (1962) and Dugdale (1960) to represent the nonlinear process located at the front of the crack.

In 1976 Hillerborg et al. extended the concept of cohesive crack for concrete (fictitious crack)

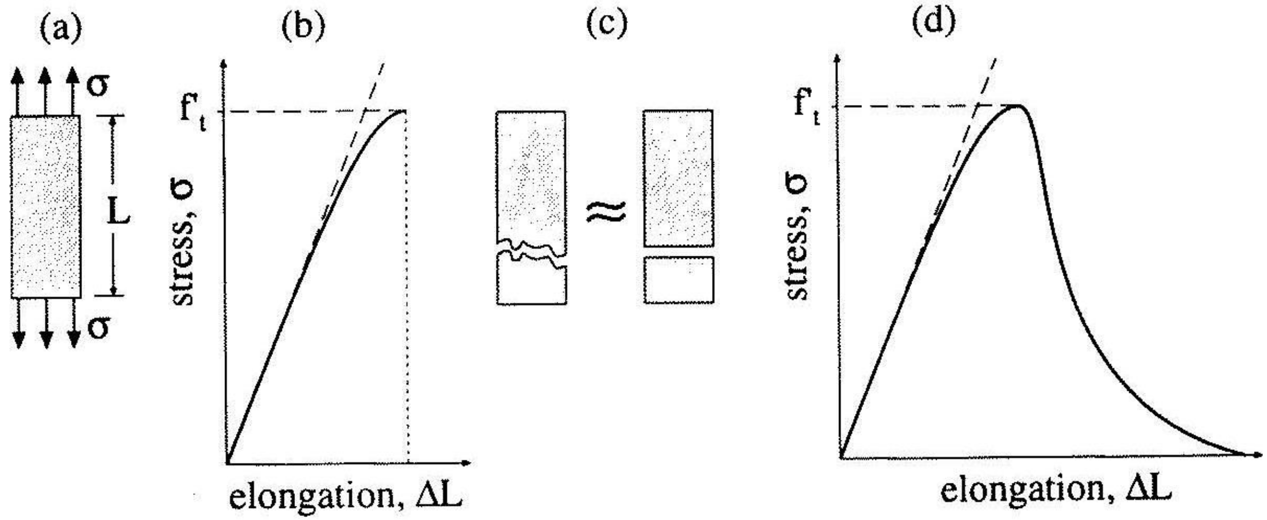

Cohesive Crack Model

Hillerborg considered two essential points:

1) After the peak all the deformation (almost) localizes into the crack
2) The evolution of the crack without a pre-existing crack

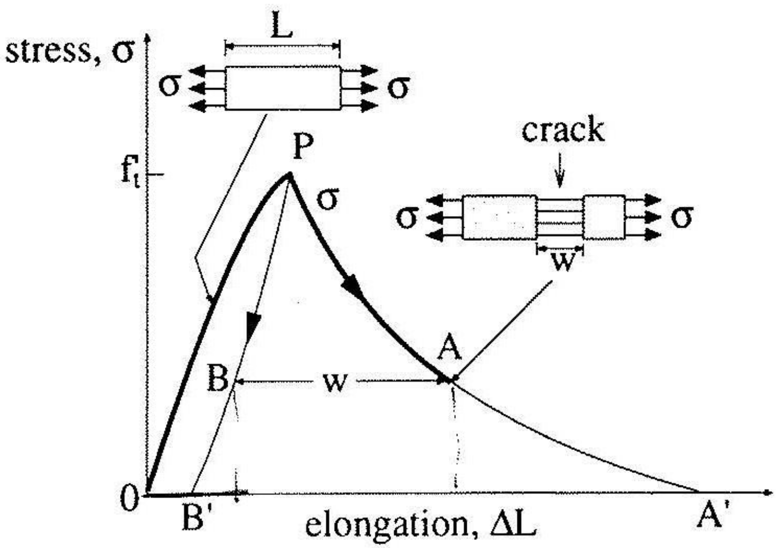

$$\Delta L = L\varepsilon_B + w$$

Cohesive Crack Model

The softening curve is the main ingredient of the cohesive crack model!

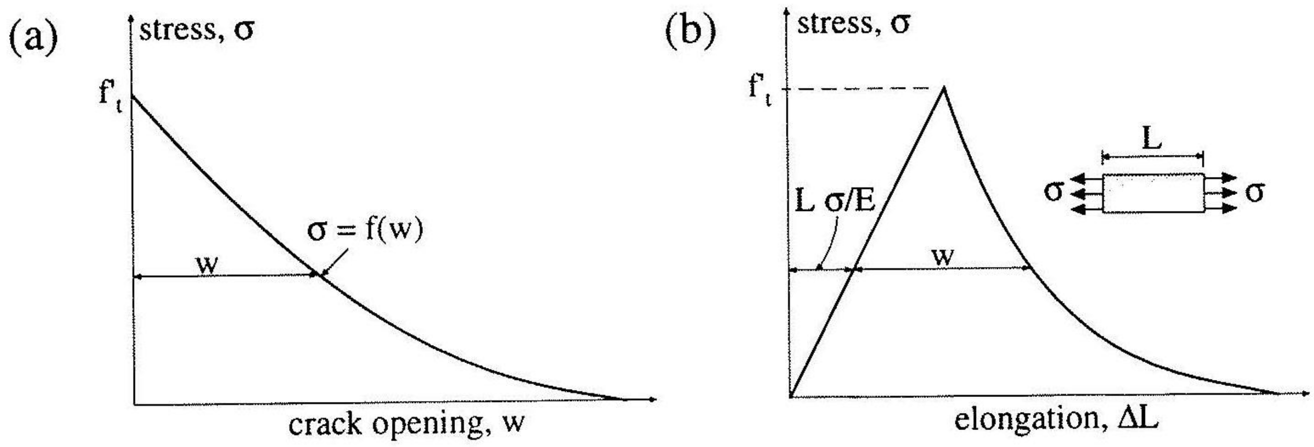

The cohesive fracture energy is the external energy supply required to create and fully break a unit surface area of cohesive crack

$$\boxed{G_F = \int_0^{\infty} f(w)\,dw}$$

Christian Carloni
cxc966@case.edu

Non-Linear Elastic Fracture Mechanics

Let's consider softening

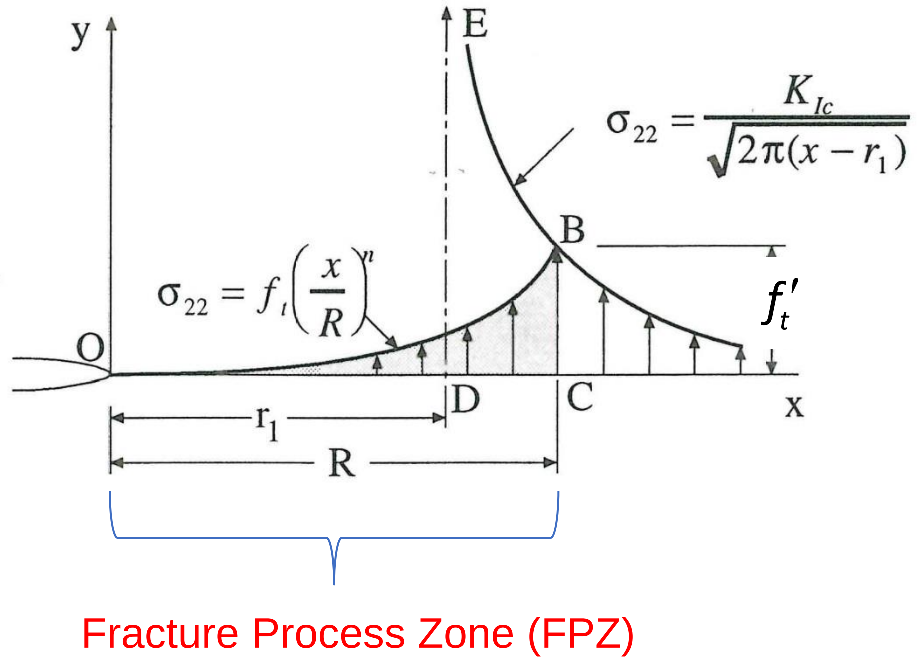

$$R = \frac{n+1}{\pi}\left(\frac{K_I}{f_t'}\right)^2$$

Non-Linear Elastic Fracture Mechanics

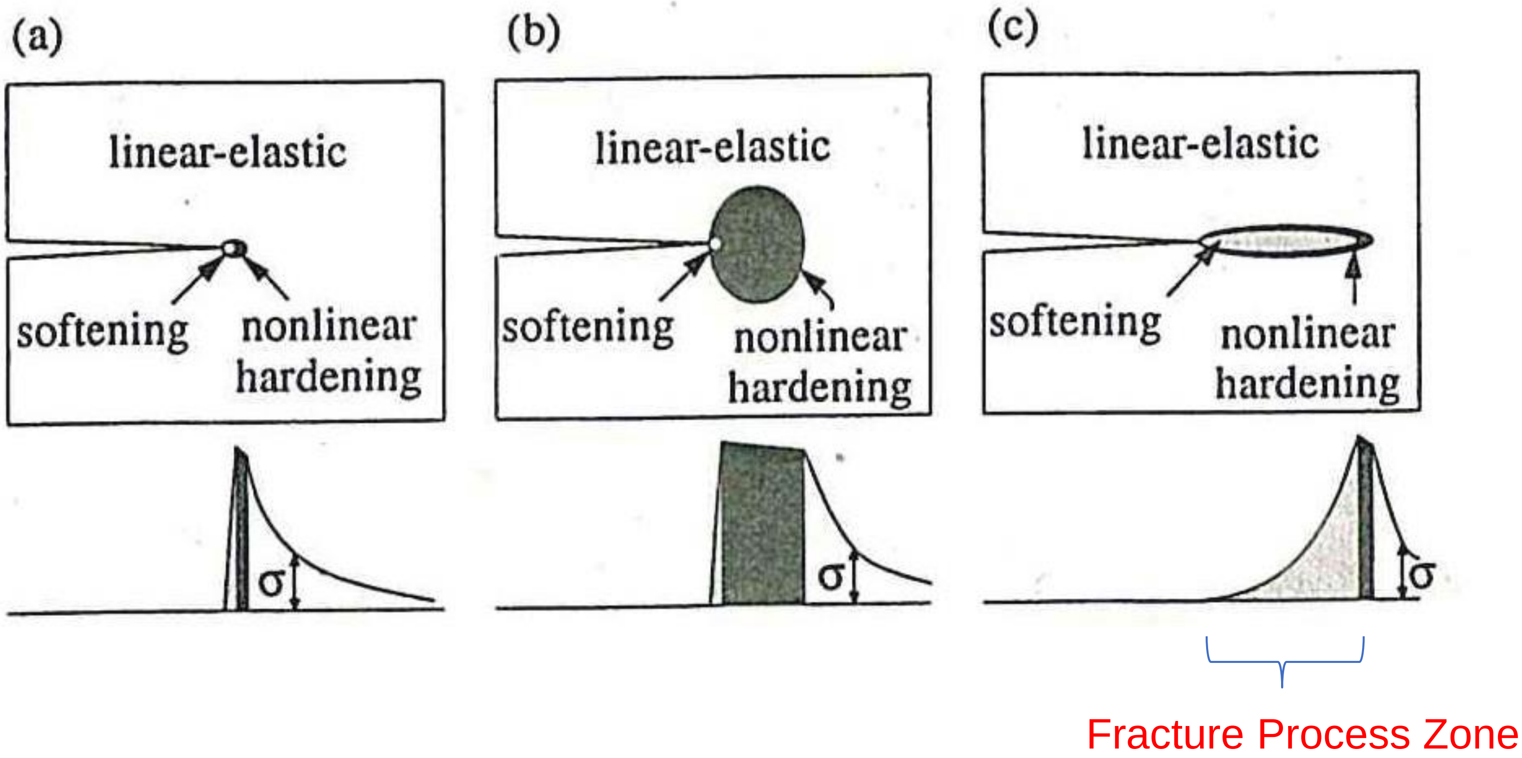

Christian Carloni
cxc966@case.edu

Size Effect

Progress in the modeling of concrete fracture and introduction of fracture concepts into design codes and practice has been impeded by the unavailability of a comprehensive database for fracture alone. The literature features a vast number of fracture data, but they all cover only rather limited ranges of specimen size, initial notch depth, and postpeak response and have been performed on different concretes, on different batches of supposedly the same concrete, at different ages, at different environmental conditions, at different rates, with different test procedures, and on specimens of different types and dimensions. **Combining all these data produces a database with enormous scatter and makes the modeling highly ambiguous because the effect of these differences is understood much less than the fracture itself.**

According to linear elastic fracture mechanics (LEFM), which applies to homogeneous perfectly brittle materials, and for geometrically similar structures with similar cracks

$$\boxed{\sigma_N \propto \frac{1}{\sqrt{D}}}$$

$$K_{Ic} = \sigma_N \sqrt{D} k(\alpha)$$

This is the strongest possible size effect

Christian Carloni
cxc966@case.edu

Size Effect

For quasi-brittle materials such as concrete, one can distinguish two simple types of size effect.

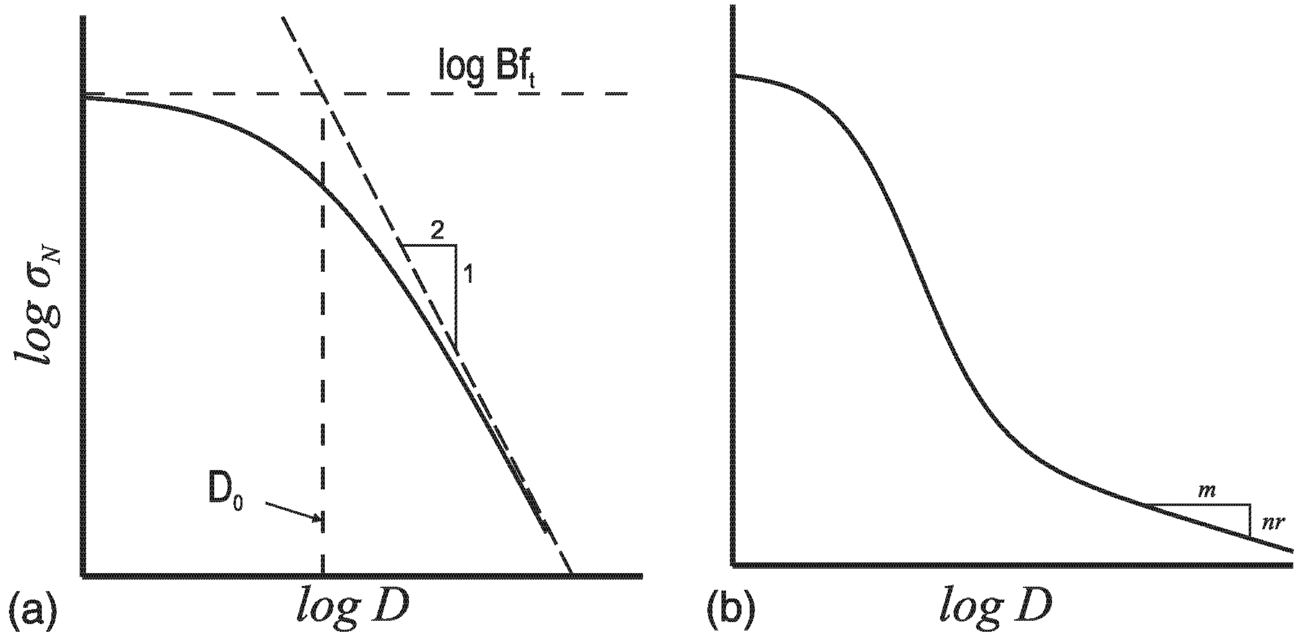

$$\boxed{\sigma_N = \frac{Bf_t'}{\sqrt{1+\frac{D}{D_0}}}}$$

Type II

Type I

Christian Carloni
cxc966@case.edu

Size Effect

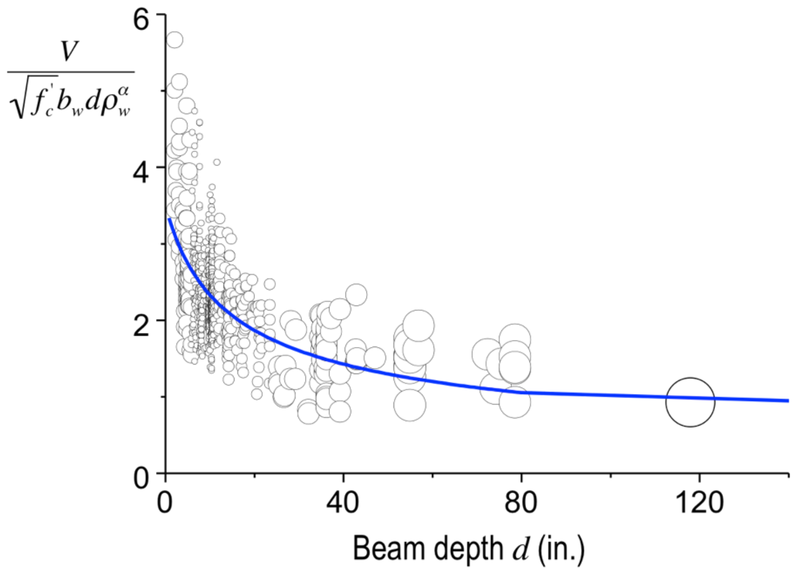

For nonprestressed members, V_c shall be calculated in accordance with Table 22.5.5.1 and 22.5.5.1.1 through 22.5.5.1.3.

Table 22.5.5.1—V_c for nonprestressed members

Criteria	V_c		
$A_v \geq A_{v,min}$	Either of:	$\left[2\lambda\sqrt{f_c'} + \frac{N_u}{6A_g}\right]b_w d$	(a)
		$\left[8\lambda(\rho_w)^{1/3}\sqrt{f_c'} + \frac{N_u}{6A_g}\right]b_w d$	(b)
$A_v < A_{v,min}$	$\left[8\lambda_s\lambda(\rho_w)^{1/3}\sqrt{f_c'} + \frac{N_u}{6A_g}\right]b_w d$		(c)

Notes:
1. Axial load, N_u, is positive for compression and negative for tension.
2. V_c shall not be taken less than zero.

$$\sigma_N = \frac{Bf_t'}{\sqrt{1+\frac{D}{D_0}}}$$

22.5.5.1.3 The size effect modification factor, λ_s, shall be determined by

$$\lambda_s = \sqrt{\frac{2}{1+\frac{d}{10}}} \leq 1 \qquad (22.5.5.1.3)$$

Experimental work

Coarse aggregate: Carey Limestone, with the maximum aggregate diameter of 10 mm

Water-cement ratio: 0.4

Entrapped air: 2.5%

Two slump tests were performed, one of them at the beginning of the casting process (114.3 mm) and the second at the end (69.85 mm).

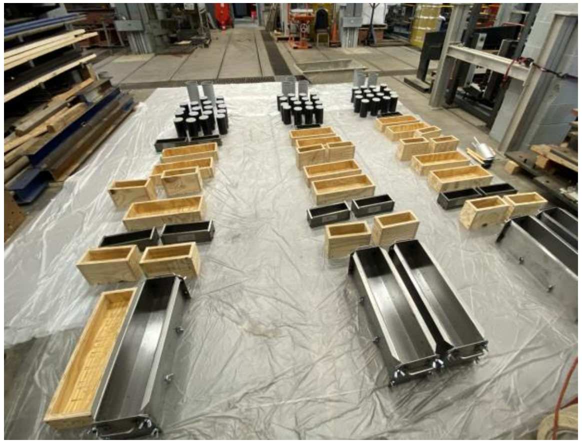

Casting date: 11/22/2019

Three-point bending tests of notched beams

5 depths were tested: 75 mm, 150 mm, 250 mm, 500 mm, 1000 mm

Christian Carloni
cxc966@case.edu

Material

$$f_{ctm}(t) = 3.6\left(\left(\exp\left\{0.386\left[1-\left(\frac{28}{t}\right)^{1/2}\right]\right\}\right)\right)^{2/3}$$

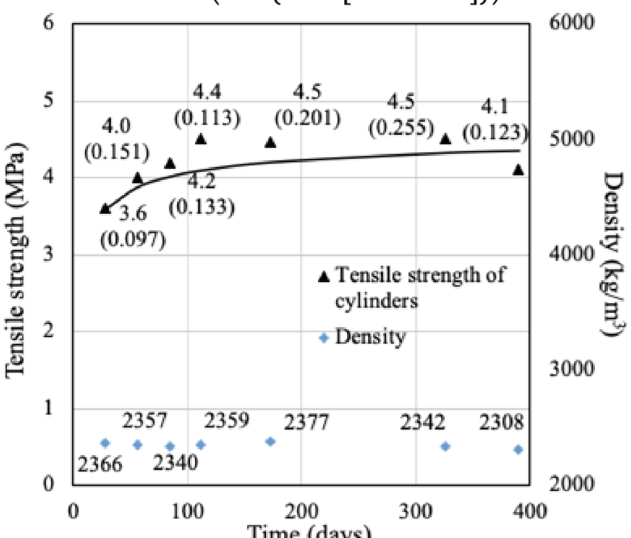

Days	Average elastic modulus (GPa) (CoV%)
28	30.2 (1.74%)
56	32.2 (4.09%)
84	33.8 (1.66%)
112	34.7 (3.43%)

$$f_{cm}(t) = 44.7\exp\left\{0.386\left[1-\left(\frac{28}{t}\right)^{1/2}\right]\right\}$$

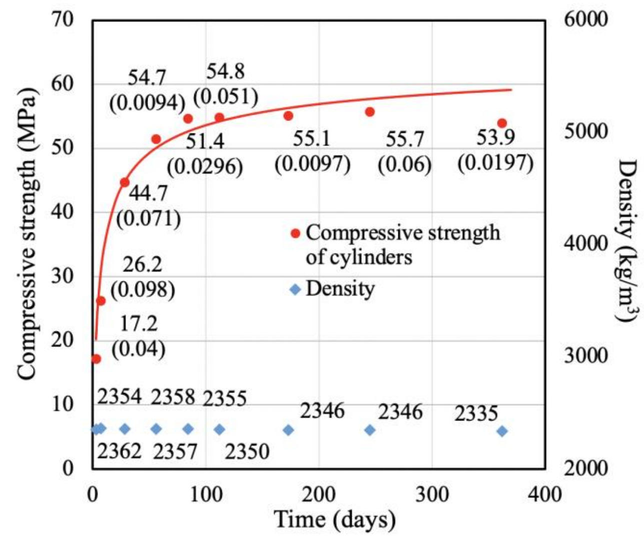

Christian Carloni
cxc966@case.edu

Test setup

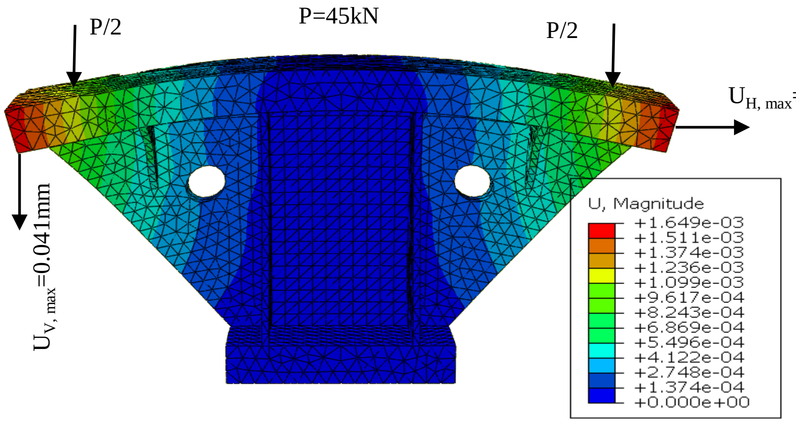

P/2
P=45kN
P/2
$U_{H,\,max}$=0.0043mm
$U_{V,\,max}$=0.041mm
U, Magnitude
+1.649e-03
+1.511e-03
+1.374e-03
+1.236e-03
+1.099e-03
+9.617e-04
+8.243e-04
+6.869e-04
+5.496e-04
+4.122e-04
+2.748e-04
+1.374e-04
+0.000e+00

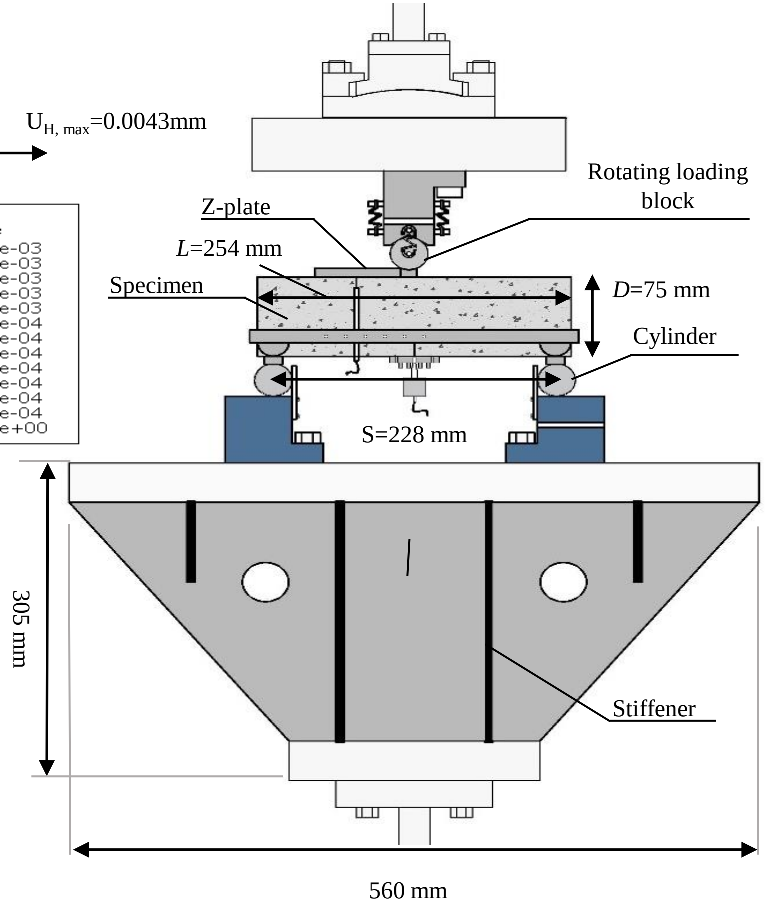

Rotating loading block
Z-plate
L=254 mm
Specimen
D=75 mm
Cylinder
S=228 mm
305 mm
Stiffener
560 mm

Test setup

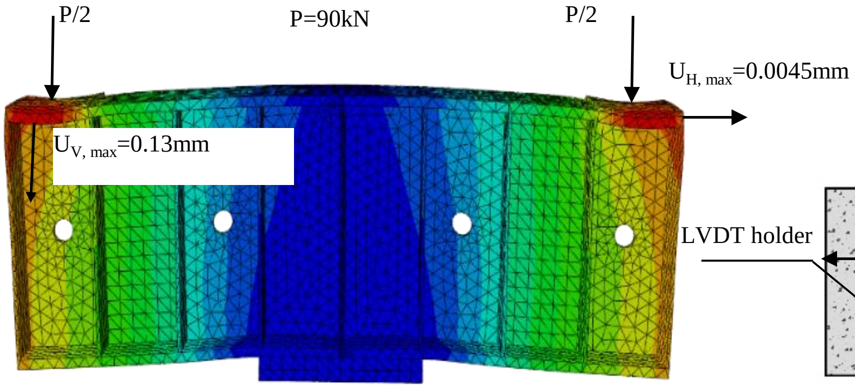

P/2
P=90kN
P/2
$U_{H,\ max}$=0.0045mm
$U_{V,\ max}$=0.13mm

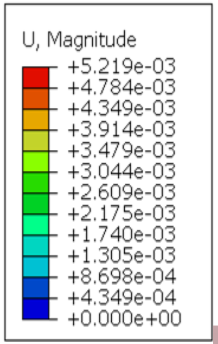

U, Magnitude
+5.219e-03
+4.784e-03
+4.349e-03
+3.914e-03
+3.479e-03
+3.044e-03
+2.609e-03
+2.175e-03
+1.740e-03
+1.305e-03
+8.698e-04
+4.349e-04
+0.000e+00

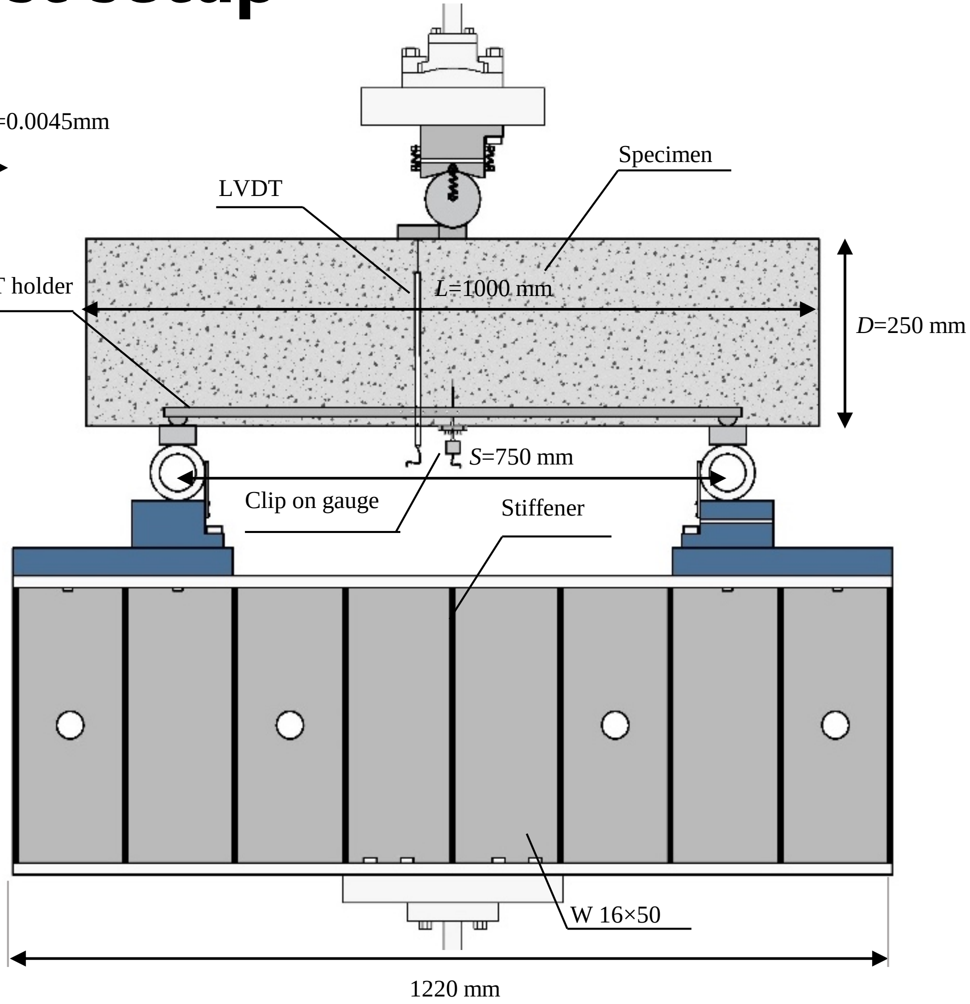

Specimen
LVDT
LVDT holder
L=1000 mm
D=250 mm
S=750 mm
Clip on gauge
Stiffener
W 16×50
1220 mm

Test setup

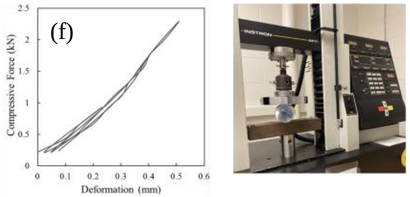

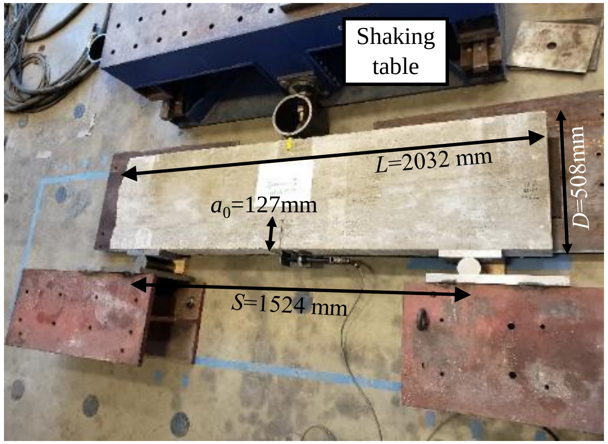

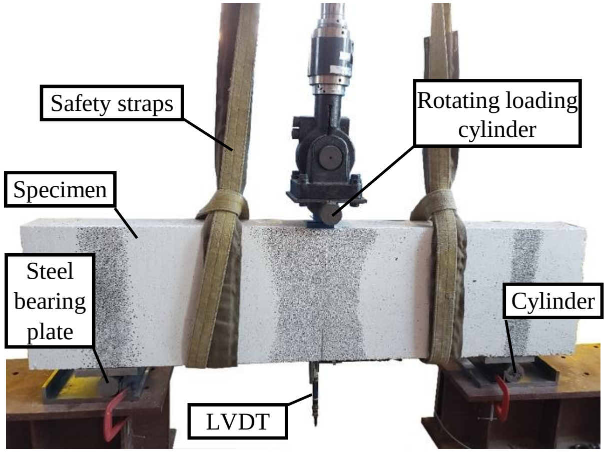

Specimen Depth = 500 mm

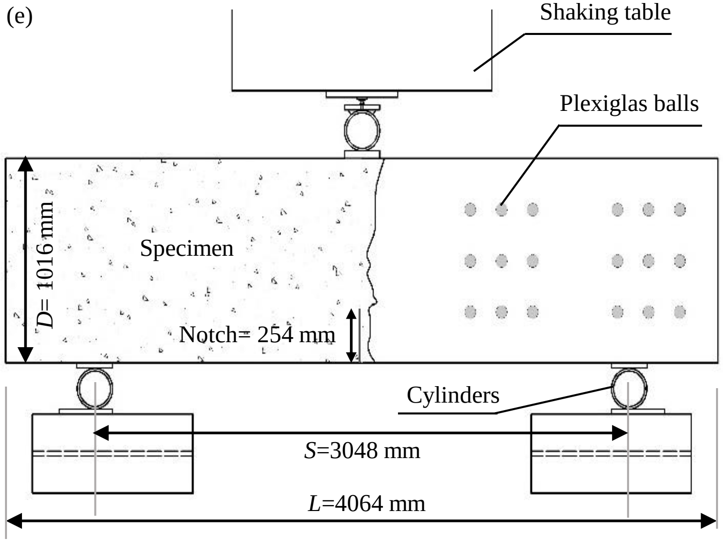

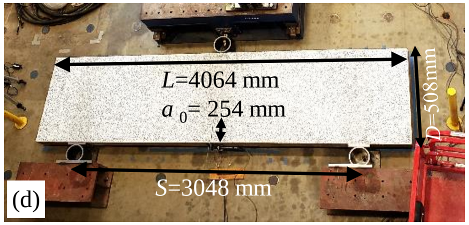

Specimen Depth = 1000 mm

Concrete Specimen After Test:

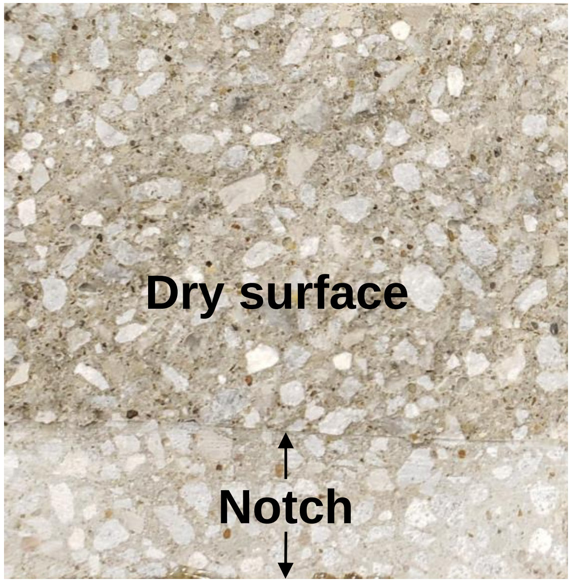

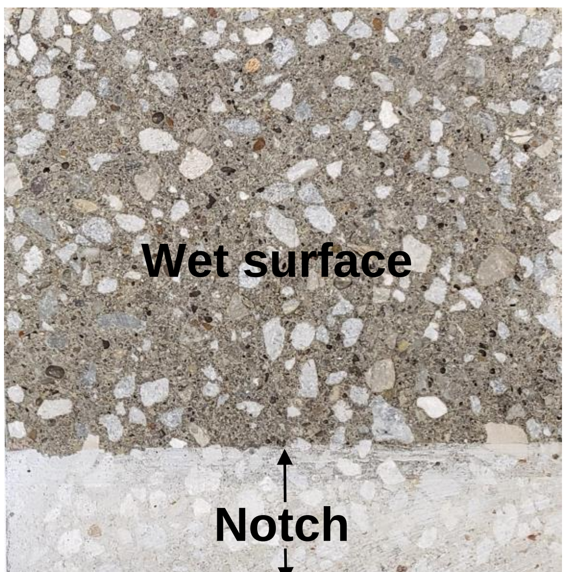

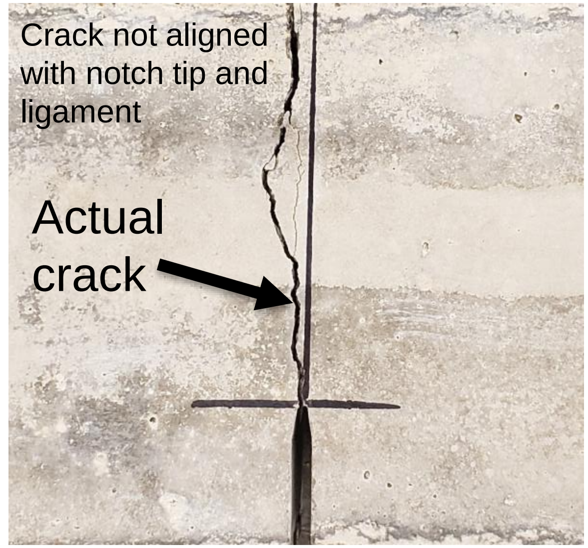

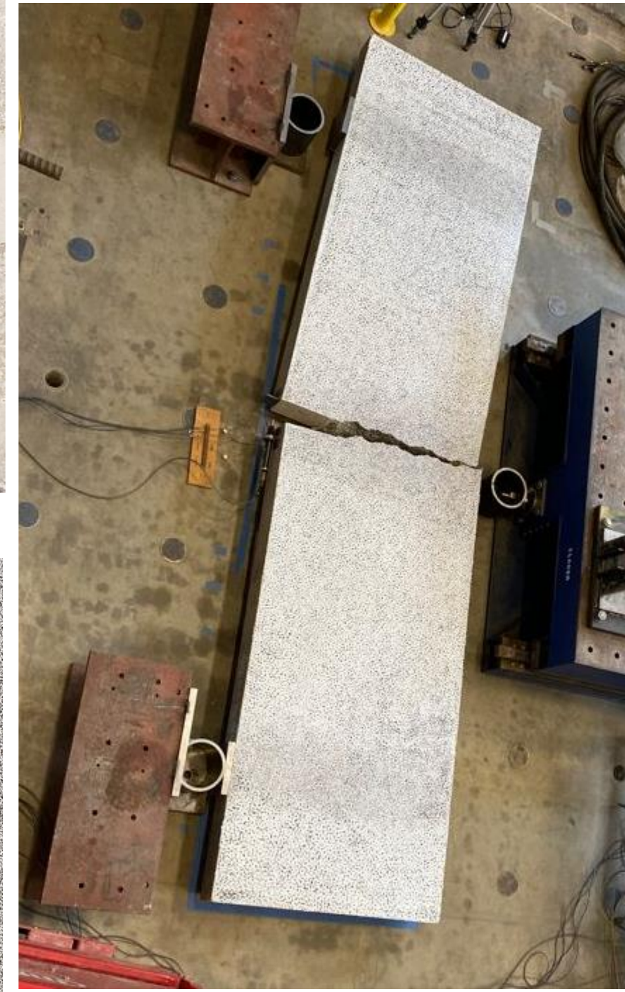

Specimen Depth =1000 mm

Christian Carloni
cxc966@case.edu

Load responses (*P*-CMOD)

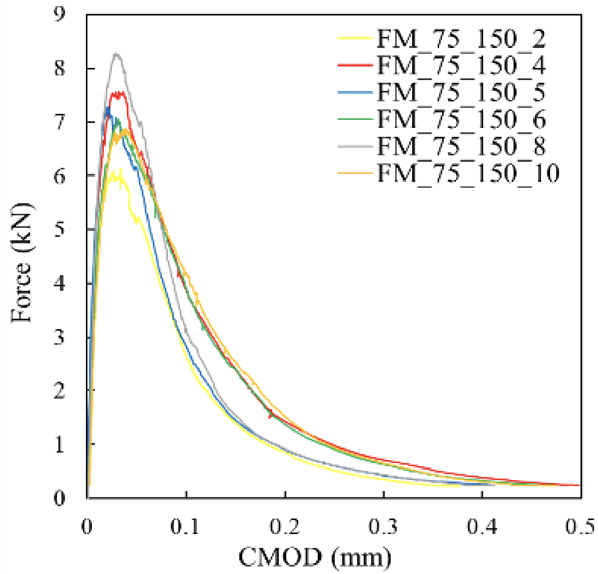

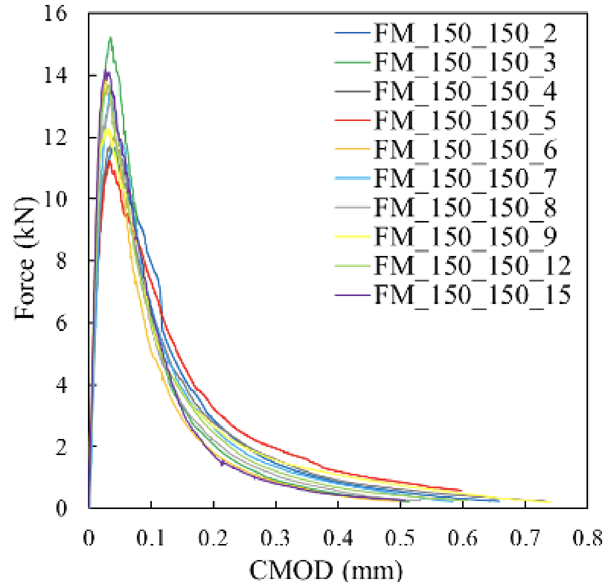

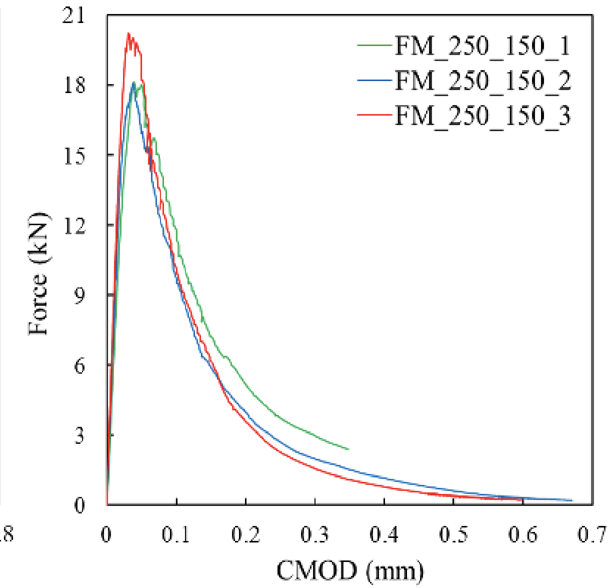

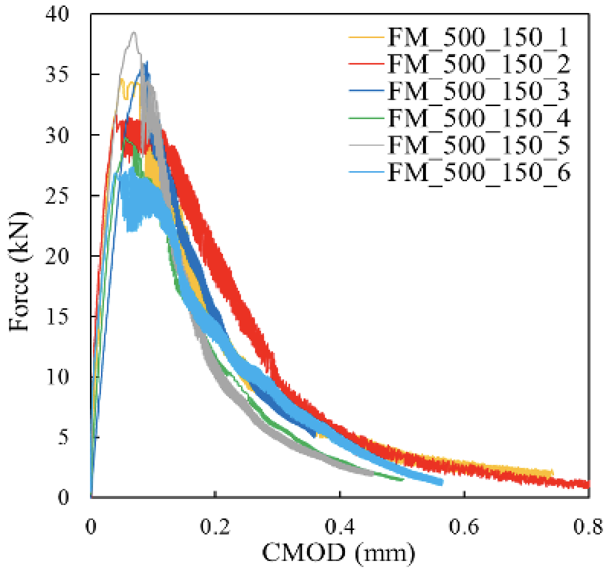

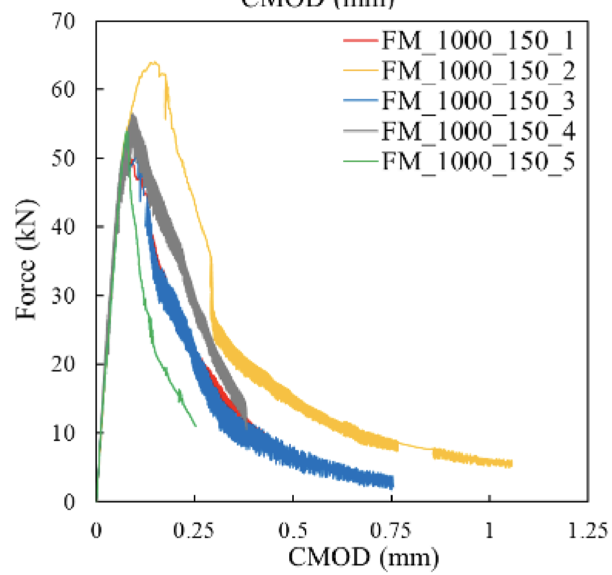

FM_D_B_x

- FM → Fracture mechanics
- D → Depth
- B → Width
- x → Specimen number

CMOD Calculations of elastic modulus

$$\omega_M(CMOD) = \frac{4\sigma_N a}{E'}\upsilon_\beta(\alpha) = \frac{6PSa}{E'BD^2}\upsilon_\beta(\alpha)$$

$$\upsilon_\beta(\alpha) = 0.8 - 1.7\alpha + 2.4\alpha^2 + \frac{0.66}{(1-\alpha^2)} + \frac{4}{\beta}(-0.04 - 0.58\alpha + 1.47\alpha^2 - 2.04\alpha^3)$$

$$\Rightarrow \quad E'_{(CMOD)} = \frac{6PSa}{\omega_M BD^2}\upsilon_\beta(\alpha)$$

Days	Average elastic modulus (GPa) (CoV)
28	30.2 (1.74%)
56	32.2 (4.09%)
84	33.8 (1.66%)
112	34.7 (3.43%)

Specimens	E'_{CMOD} (GPa)
FM_75_150_x	30.9
FM_150_150_x	32.3
FM_250_150_x	34.5
FM_500_150_x	34.1
FM_1000_150_x	37.8

Christian Carloni
cxc966@case.edu

Load responses (P-δ)

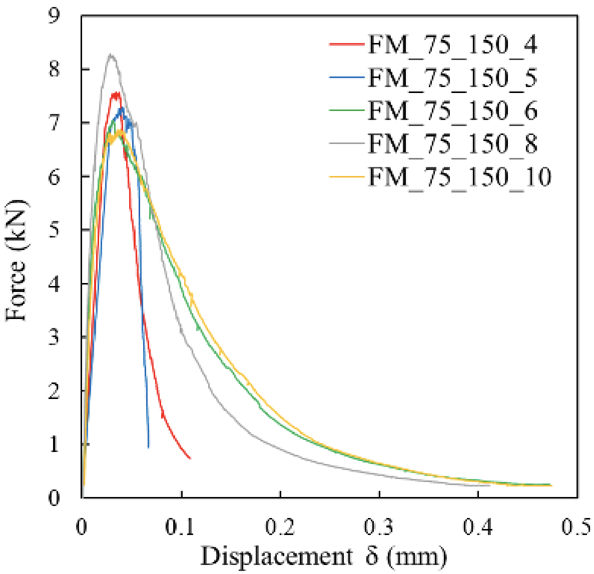

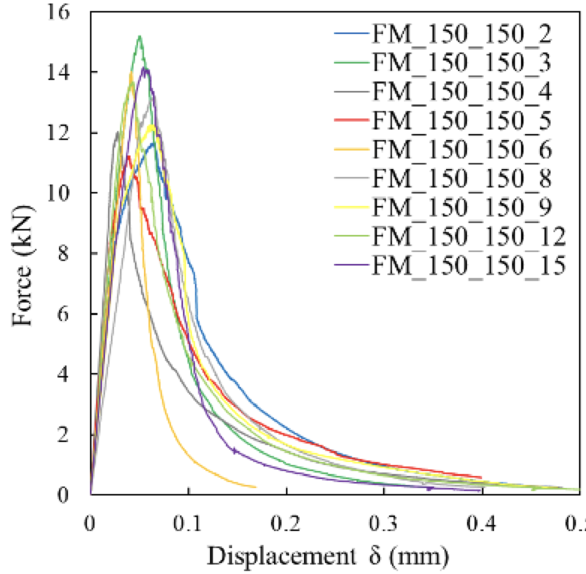

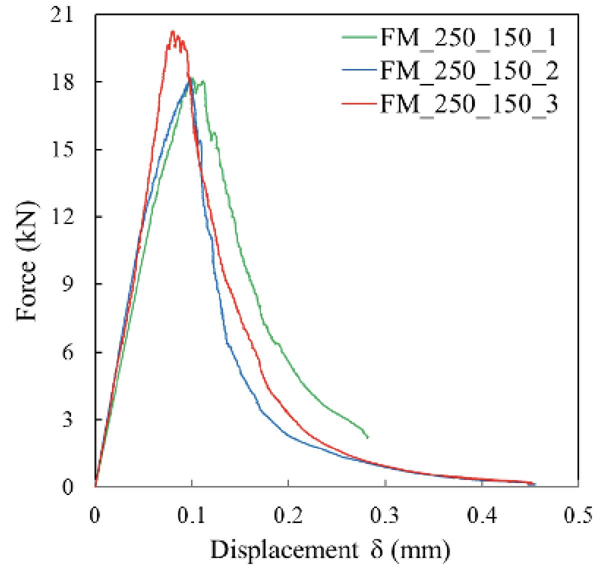

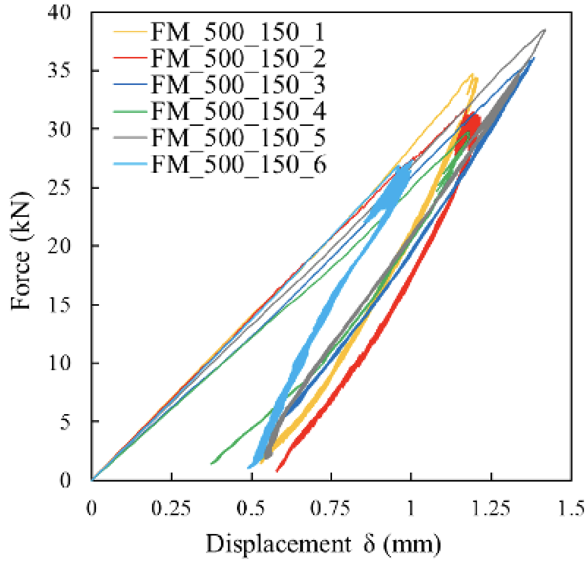

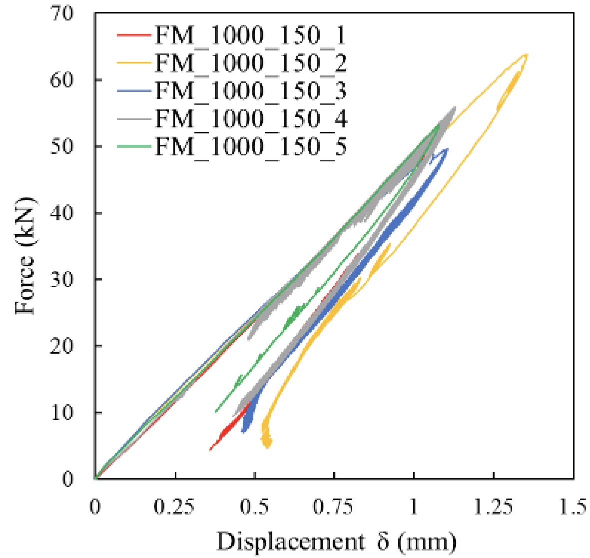

Fracture Energy, G_F

Specimens	G_F (N/m)
FM_75_150_x	49.29
FM_150_150_x	83.10
FM_250_150_x	99.20
FM_500_150_x	153.51
FM_1000_150_x	93.68

Specimens tested with higher rate (20x)	G_F (N/m)
FM_75_150_x	57.76
FM_150_150_x	107.99
FM_250_150_x	129.04

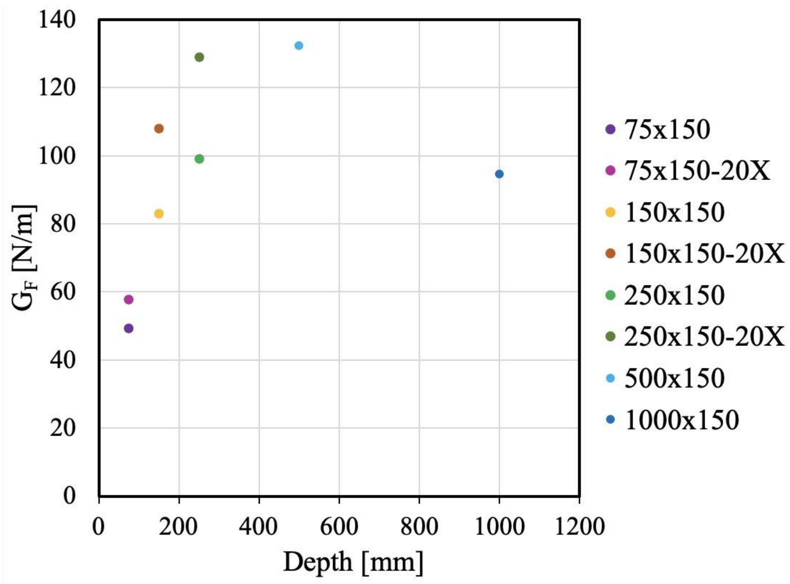

Digital image correlation (DIC): Setup

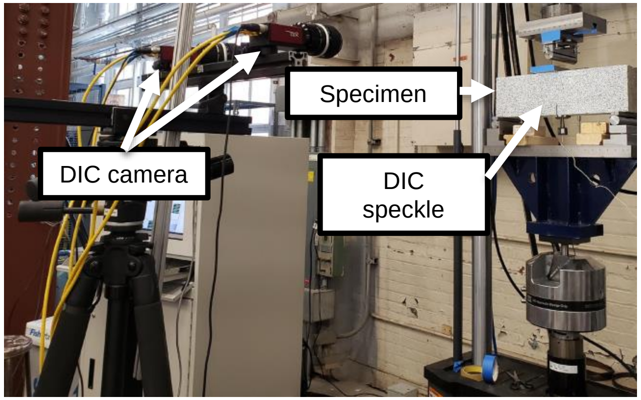

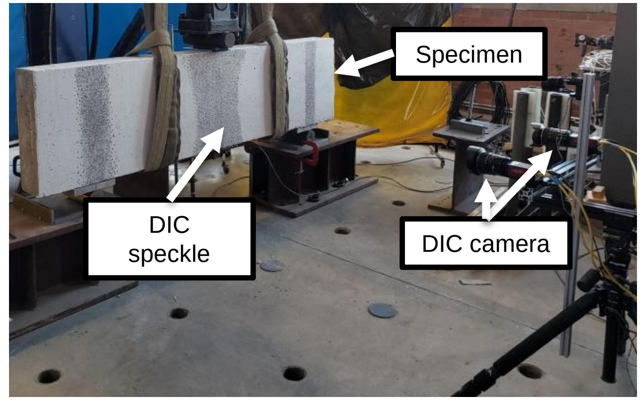

DIC setup for specimens of depth = 500 mm

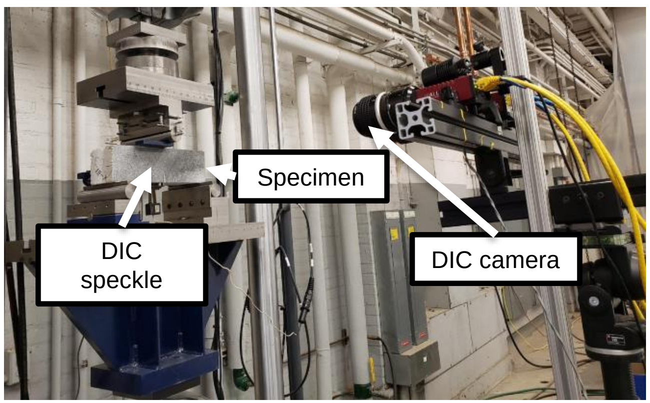

DIC setup for specimens of depth ≤ 250 mm

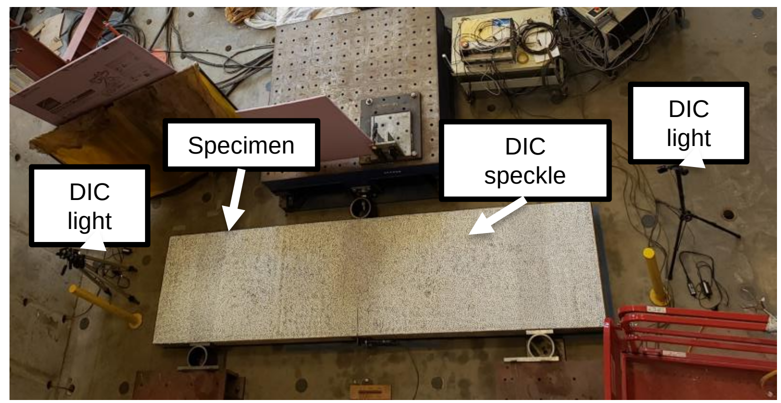

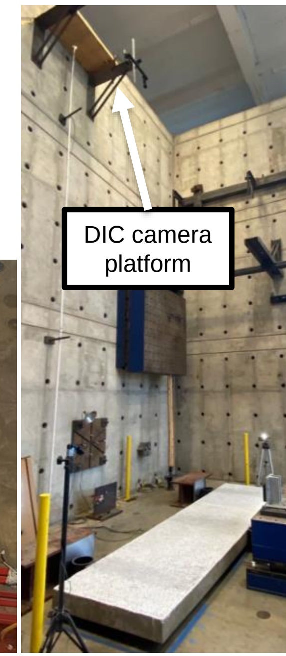

DIC setup for specimens of depth = 1000 mm

DIC analysis: Specimen FM 75_150_6 (Subset - 41; Step - 10)

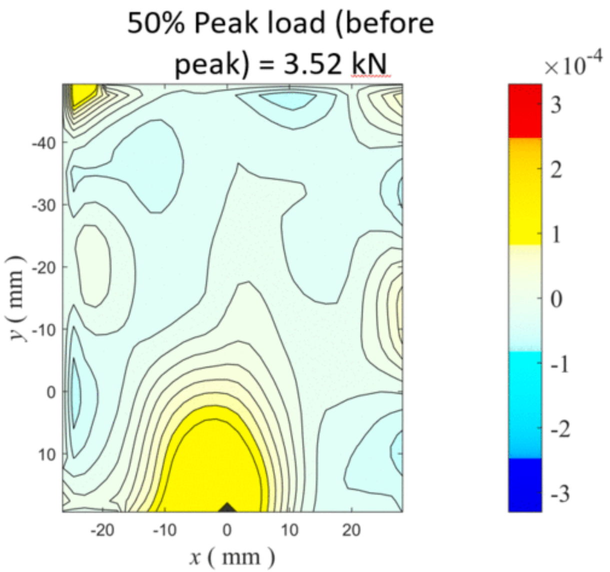

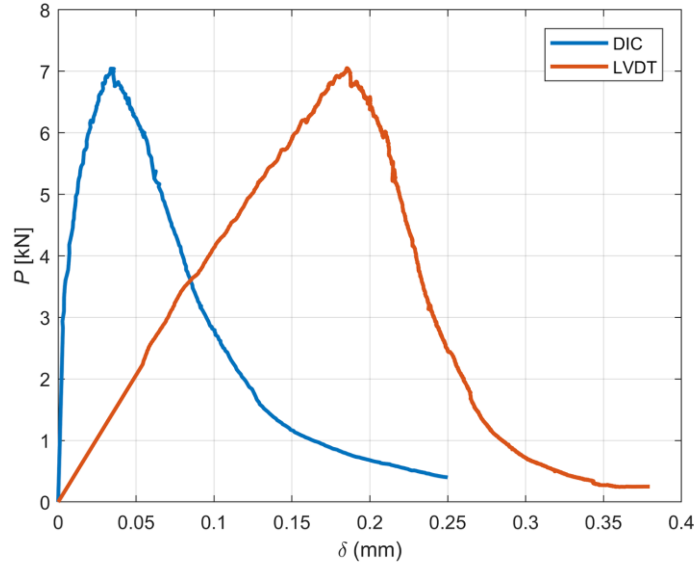

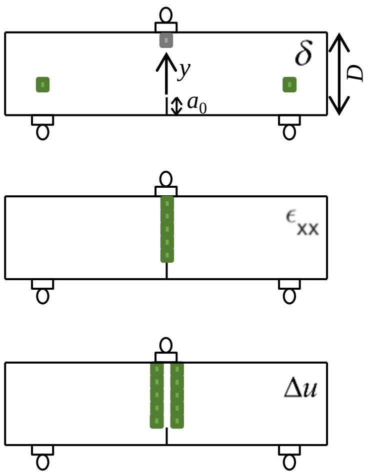

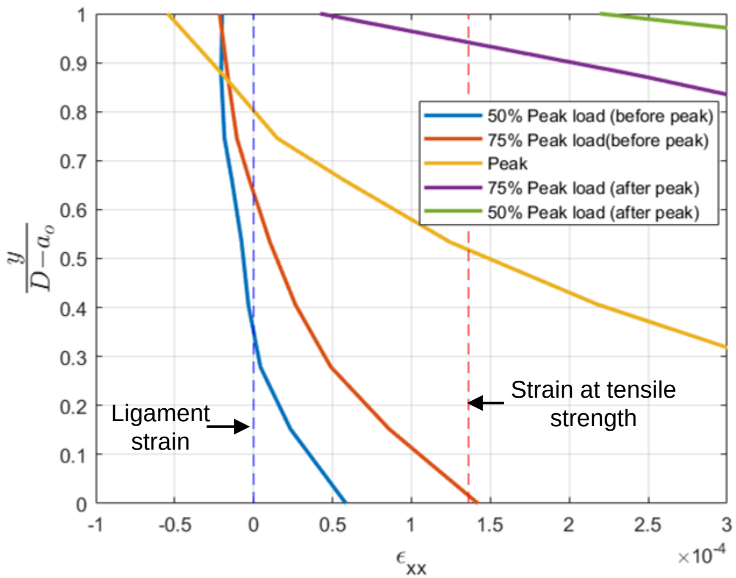

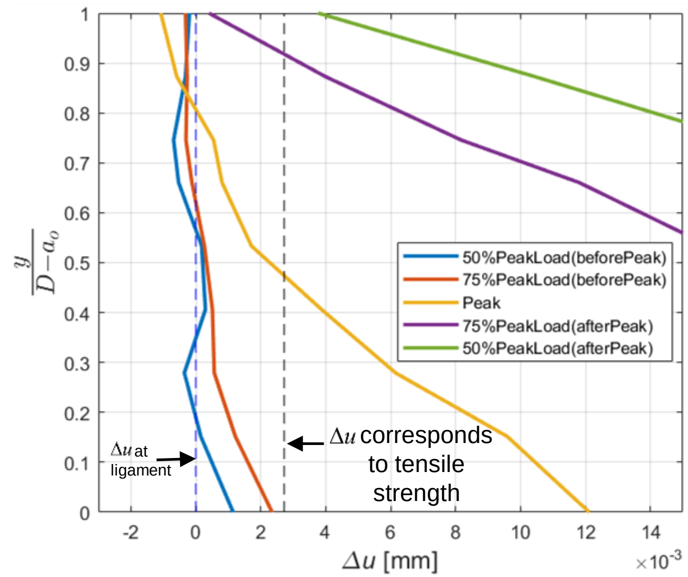

Christian Carloni
cxc966@case.edu

Baietti, G., Quartarone G., Carabba, L., Manzi, S., Carloni C., Bignozzi, M.C. (2020). Use of Digital Image Analysis to Determine Fracture Properties of Alkali-Activated Mortars. Engineering Fracture Mechanics, 240, https://doi.org/10.1016/j.engfracmech.2020.107313

Size Effect Curve

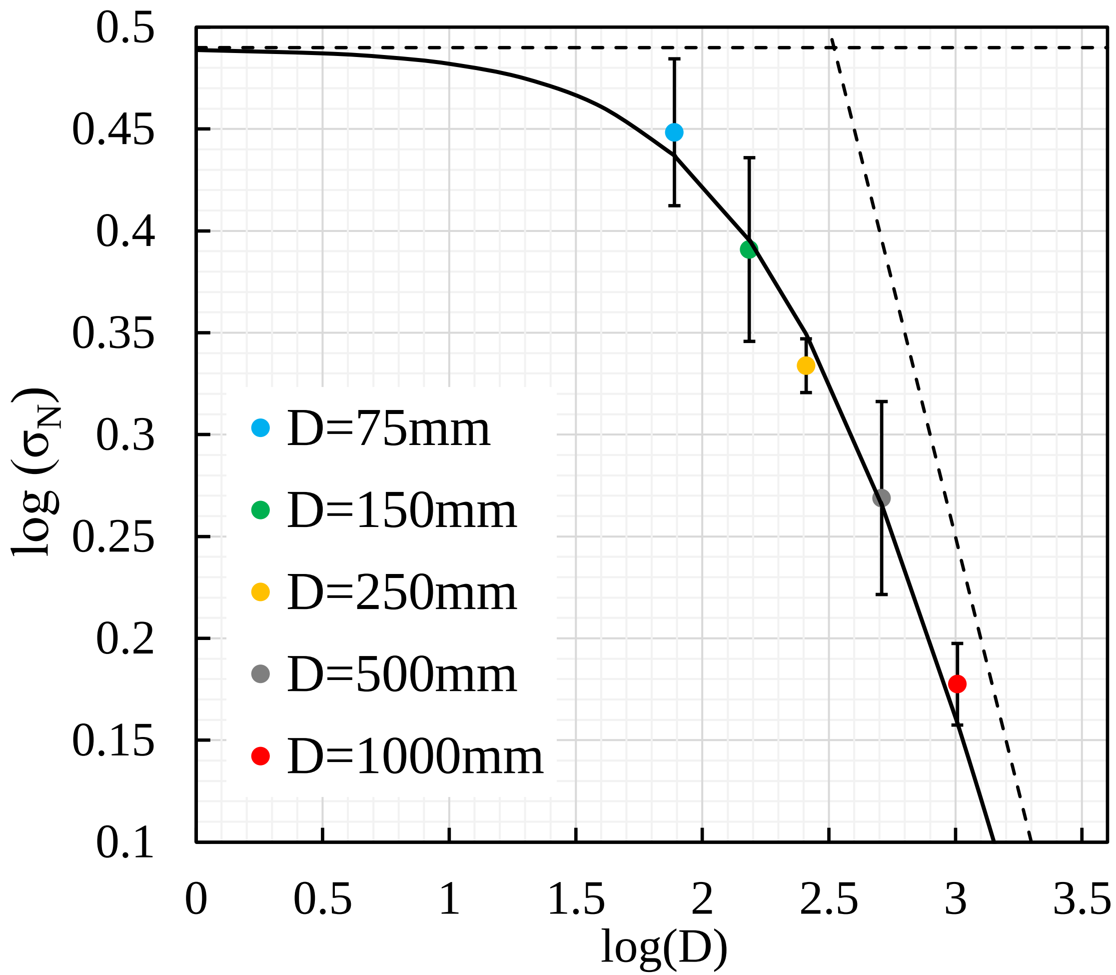

Christian Carloni
cxc966@case.edu

How to model

- Cohesive crack model is a good tool
- Lattice Discrete Particle Model
- Other numerical models
- Cohesive hinge

Christian Carloni
cxc966@case.edu

Cohesive Hinge Model

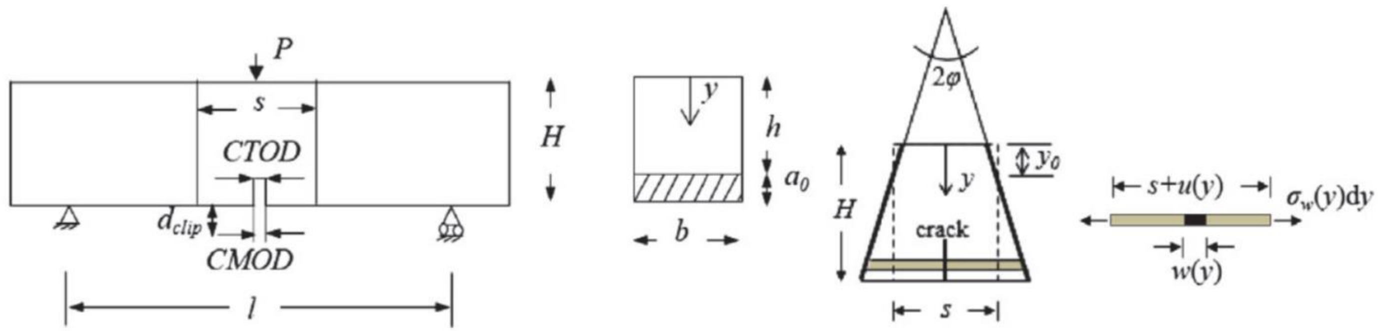

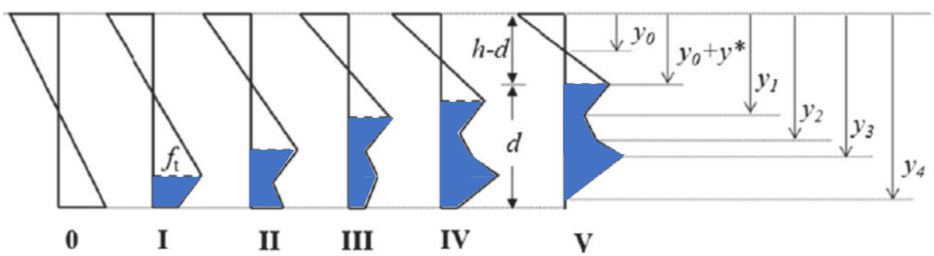

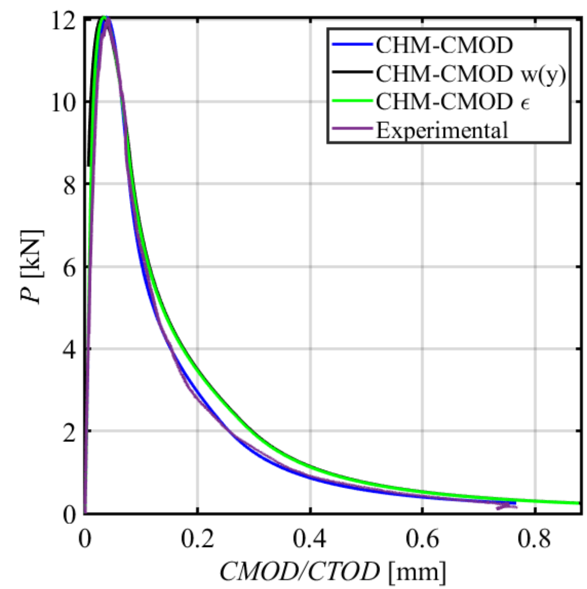

CASE SCHOOL OF ENGINEERING
CASE WESTERN RESERVE UNIVERSITY

Christian Carloni
cxc966@case.edu

Cohesive hinge model

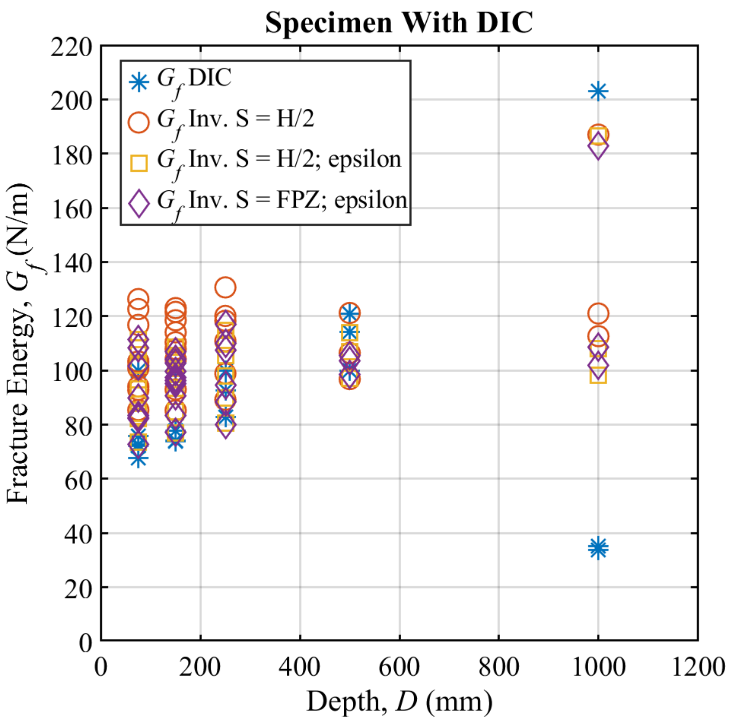

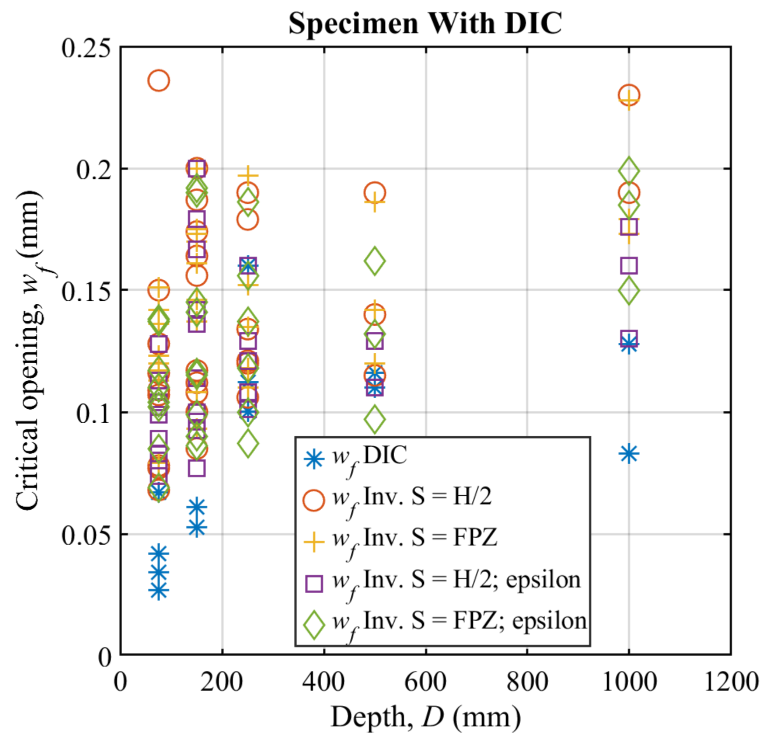

What if I have a structure with fixed ends?

Conclusions

- Fracture mechanics can be used to predict size effect
- Material properties can be obtained from size effect tests
- DIC analysis used to determine the size of the FPZ
- Size effect plot confirms the trend of SEL
- A cohesive hinge model can be calibrated to determine the size effect trend

Christian Carloni
cxc966@case.edu

What is in the future

- Test even larger sizes or thicker elements
- The test method can be extended to shear strength of plain concrete
- Different concretes can be studied to analyze the effect of aggregates and effect of SCM

Christian Carloni
cxc966@case.edu

Thank You!

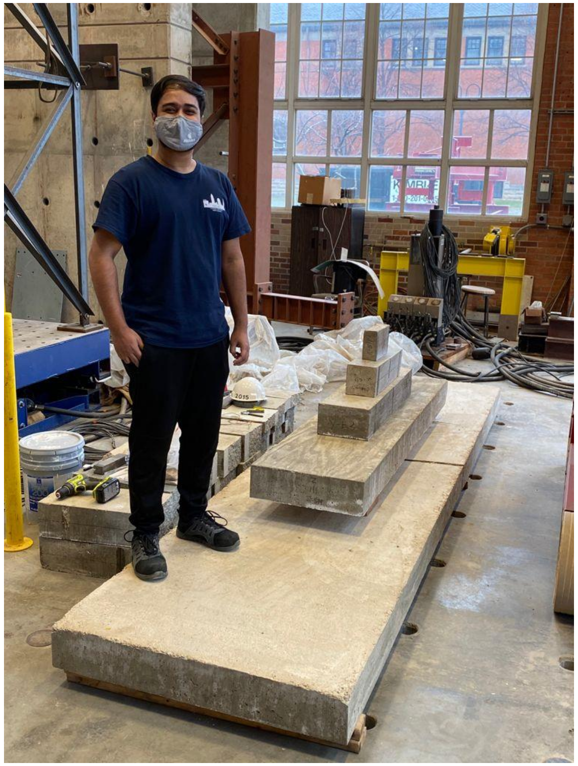

Christian Carloni
cxc966@case.edu